Title
Remote isotope detection and quantification using femtosecond filament-laser ablation molecular isotopic spectrometry

Authors
Chirinos, Jose
Spiliotis, Alexandros
Mao, Xianglei
et al.

Publication Date
2021-05-01

DOI
10.1016/j.sab.2021.106117

Peer reviewed

Remote Isotope Detection and Quantification using Femtosecond Filament-Laser Ablation Molecular Isotopic Spectrometry

Jose Chirinos[a], Alexandros Spiliotis[a,b,c], Xianglei Mao[a], George C.-Y. Chan[a], Richard E. Russo[a,d], Vassilia Zorba[a,e,*]

a. *Lawrence Berkeley National Laboratory, Berkeley, CA 94720,USA.*
b. *Institute of Electronic Structure and Laser, Foundation for Research and Technology Hellas, 71110 Heraklion-Crete, Greece.*
c. *Department of Physics, University of Crete, 71003 Heraklion-Crete, Greece.*
d. *Applied Spectra, Inc, West Sacramento, CA 95605, USA.*
e. *University of California, Berkeley, CA 94720, USA.*

Abstract

We demonstrate the detection and quantification of isotopes from solid samples remotely at a distance of 36 m. This was accomplished through the combination of femtosecond filaments and laser ablation molecular isotopic spectrometry (F^2-LAMIS). Isotopically enriched graphite samples with varying ^{13}C concentration were used and the F^2-LAMIS emission was measured remotely using a portable spectrometer system. A standardless quantification approach was used to determine the corresponding isotopic ratios. The use of F^2-LAMIS for the detection and quantification of isotopes at atmospheric pressure without the use of calibration standards opens the possibility to implement this technology for remote sensing of isotopes in field applications.

Keywords: Remote isotope detection, F^2-LAMIS, femtosecond filament, isotope ratio, standardless quantification

*Corresponding author: vzorba@lbl.gov

1. Introduction

Laser Induced Breakdown Spectroscopy (LIBS) and Laser Ablation Molecular Isotopic Spectrometry (LAMIS) are very attractive spectrochemical techniques due to their ability to perform real-time analysis at atmospheric pressure with no sample preparation. LIBS can analyze optical emission from excited atoms and ions in the ablation plume when the plasma is hot and provide information predominantly about the elemental composition of samples. In contrast, LAMIS can detect isotopes by analyzing molecular emission as the plasma cools by taking advantage of the relatively large isotope shifts in spectra of transient molecular isotopologues. [1-3].

There is growing interest to use LAMIS at remote distances for difficult to access or hazardous environments, as well as in space exploration missions. The detection of isotopes in solid samples at distance represents a significant challenge, and there is a lack of technologies to enable this application. Conventional nanosecond lasers for standoff laser plasma generation is limited by the difficulty to tightly focus the beam at long distances. Optical diffraction limits sufficient laser fluence for the ablation process at long range, demanding the use of very high laser energies [4]. Ultrashort laser pulses provide an alternative for remote laser plasma generation as their self-

focusing capability can overcome diffraction and ensure long propagation, while retaining most of the peak power. Such laser beams can propagate many meters with almost constant high peak intensity due the well-known filamentation effect [5]. Filamentation is defined as a long plasma channel produced by the dynamic balance between Kerr self-focusing and defocusing of the plasma generated in air. Filaments have a central core with diameter on the order of 100 μm an energy reservoir that is more than 5 times the diameter of the core and contains approximately 50% of the beam energy [6]. When self-focusing is saturated, the pulse energy collapses to a thin filament, with a clamped peak intensity of about 40 TW/cm^2, enough to ablate solid samples and induce high-intensity plasma emission [5-8].

Elemental analysis using Remote LIBS has been reported with Terawatt lasers [9,10]. Specifically, LIBS emission from filament-induced plasmas on Cu and Fe targets were detected at 90 m with 250 mJ fs laser pulses with wavelength of 800 nm. The analysis of Al alloy was recorded at 50 [11] and 60 m distances [12], including under extreme environmental conditions such as such as extreme pressure or temperature gradients [12]. Elemental signals from complex biological samples were also detected at short distance (less than 6 m) using a Ti:Sapphire laser system at several mJ of energy [13-14].

For isotopic analysis at a distance, Femtosecond Filament - Laser Ablation Molecular Isotopic Spectrometry (F^2-LAMIS), a technology which combines filamentation with the LAMIS technology, has been reported for Zr isotopic analysis [15]. Using F^2-LAMIS, it was possible to detect and quantify the natural isotopic abundance of ^{90}Zr, ^{91}Zr, ^{92}Zr and ^{94}Zr with the sample positioned at 8 m, and collecting the molecular oxide emission close to the plasma. A fitting algorithm was used in this case for standardless quantification [15]. The detection of uranium oxide

isotopic shift without quantification in a ^{235}U enriched sample was achieved with the sample positioned in a chamber 1 m from the collection optics [16].

One of the challenges for isotope detection with optical spectroscopy at long distances is the difficulty to collect the plasma emission, as signals decrease in a quadratic fashion with the distance between the plasma and telescope. In addition, control of the filament is necessary to obtain an intense and stable plasma in open air, especially for less powerful lasers. Finally, isotope quantification is challenging due to lack of matrix matched calibration standards at remote distances. This work explores F^2- LAMIS for remote isotope detection and quantification at a sample-to-laser distance of 36 m, by studying ^{13}C and ^{12}C emission in isotopically enriched graphite samples. The C_2 molecular emissions were detected by a telescope and spectrometer at 36 m distance from the sample. A standardless spectral fitting approach was used to determine the ^{13}C isotopic abundance in the F^2-LAMIS spectra.

2. Experimental

The experimental system is shown in **Figure 1**. A Ti:Sapphire laser (Astrella, Coherent) with an energy of 5 mJ at 800 nm wavelength was used in this work. The laser pulse was stretched to 150 fs and the laser repetition rate ranged from 50-200 Hz. A frequency resolved optical gating or FROG system (Newport) was used to determine the pulse width and chirp. A custom refractive beam expander placed at the laser exit was used to change beam diameter and adjust the filament initiation distance. The expander consisted of two lenses with f_1 = -30 cm and f_2 = 100 cm. A

precision translation stage was used to control the distance between the lenses, which directly affected the self-focusing characteristics of the femtosecond (fs) beam.

Filament plasma generation and LAMIS isotope signal detection took place at 36 m. Gold coated mirrors were used to fold the laser beam in order to extend the beam path within the limited laboratory space available (18 m) for the beam propagation. It is important to note that the beam was folded before the filament was formed. Any interaction of the filament itself with a mirror would lead to its inadvertent ablation and damage. Using this configuration, we generated a 36 m beam path for the filament propagation and for detection. The graphite sample was placed on a rotational stage to assure reproducible ablation of the sample. The optical emission from the plasma was also collected at 36 m from the filament-induced plasma with a 20" Dobsonian Telescope, coupled to a fiber optic cable, to direct the plasma emission to a spectrometer (Isoplane 320, Princeton Instrument) with an intensified charge coupled device (ICCD, Princeton Instruments) detector. The spectrometer was equipped with a 1800 lines/mm grating, and the spectral resolution was 0.04 nm. All experiments took place in air at atmospheric pressure.

Amorphous carbon powder enriched with 99% ^{13}C (97% pure, Cambridge Isotope Laboratories) was mixed with natural abundance graphite powder to obtain 1.1%, 4.1% and 6.2% ^{13}C abundance samples after pressing them into pellets. A silicon wafer was used to characterize the filament-induced ablation craters formed. This surface is atomically flat and therefore serves as an ideal material to precisely measure the filament ablation crater properties. The number of femtosecond filament pulses interacting with the material surface was controlled by an electromechanical shutter (Uniblitz Electronic). White light interferometry (Zygo Corporation) was used to measure

the crater diameter, depth and volume. Furthermore, the surface morphology of the craters was studied using bright-field optical microscopy (BX51, Olympus Corporation).

3. Results and discussion

3.1 Prediction and control of the filament initiation distance

The first part of this study focused on optimization and control of the filament propagation and initiation distance in order to maximize the LAMIS isotopic signatures at 36 m. Typically, the self-focusing distance of femtosecond laser pulses in air can be from centimeters to several meters and strongly depends on the laser pulse duration, energy and beam spatial characteristics such as focusing [5]. Additionally, atmospheric turbulence, pressure gradients, and the presence of different gases in its path can affect the filament propagation, as well as the energy conditions for filament seeding.

In order to control the filament initiation distance and filament length for any given pulse duration and laser energy, we incorporated a custom designed beam expander. Estimation for the effective filament initiation distance *(f')* for a beam expander comprising two optics of any type is provided by **Equation 1** for an initially collimated beam [7]:

$$f' = d + f_2 \frac{Z_{sf}(f_1 - d) - d\,f_1}{Z_{sf}(f_1 + f_2) + f_1 f_2 - d\,(Z_{sf} + f_1)} \qquad (1)$$

Where, f_1 and f_2 are the focal lengths of the beam expander lenses, and d the distance between the lenses. Z_{sf} is the distance at which a filament is generated under the effect of Kerr self-focusing given by the Marburger formula (**Equation 2**) [8]:

$$Z_{sf} = \frac{0.367ka^2}{\sqrt{\left(\sqrt{\frac{P}{Pc}} - 0.852\right)^2 - 0.0219}} \quad (2)$$

Here k is the wave number and a is the laser beam radius at $1/e$. P and P_c are the peak and critical peak power of laser, respectively.

Using this formula we calculated the appropriate beam expander characteristics to form a stable filament-induced plasma at 36 m. The laser pulse was stretched to 150 fs and the repetition rate was set at 200 Hz. These conditions provided a peak power of about 35 GW that is greater than the critical power of 5 GW necessary for filamentation [7]. The length of the filament was approximately 5 m. The beam expander was then fine-tuned by monitoring the plasma to get the most intense emission from the graphite sample.

2.2 Femtosecond filament-induced surface modification

Figure 2 shows white light interferometry of a typical crater generated with a single laser pulse at 36 m on a silicon wafer. The 2D surface map is shown in **Figure 2a**, where the color scale represents the crater depth. While the diameter of the crater is in the order of hundreds of microns, the depth is only a few nanometers. Specifically, **Figure 2b** shows the crater cross section with dimensions of 363 ± 10 μm in diameter, 5.1 ± 0.4 nm in depth and 471 ± 13 μm^3 in volume. Similar results were obtained with ablation of GaAs [23]. The estimated fluence was 5 J/cm^2 with

approximately 1.1 ng of removed material based on a Si 2.33 g/cm^3 density. Accumulation of material was observed in the center of the crater, which may be attributed to melt propagation and hydrodynamic motion of liquid Si prior to solidification in high fluence regimes [24]. A secondary ring is noticed outside the crater, with a radius of about 500 μm from the center. This ring is almost at the same height as the substrate, and is most likely attributed to localized lower fluence oxide formation. This is because the filament core and energy reservoir (where the majority of the filament energy is contained) are further surrounded by the less intense portion of the beam that contains the remaining energy [23]. **Figure 3** shows optical microscopy images, demonstrating shot-to-shot ablation on the silicon surface. Spreading of the ablation area is observed with increasing number of filament pulses. This increased area is attributed to the pointing stability of the filaments in air [10,25], which leads to ablation at sightly different locations on the sample with consecutive pulses, resulting to a larger overall filament-material interaction area. The filament pointing stability is influenced by a number of parameters, including the pulse-to-pulse stability of femtosecond laser beam itself, the filament launching optics, and the propagation medium. For example, atmospheric conditions such as turbulence and pressure gradients can also affect the filament pointing stability.

3.3. Remote Isotope Measurements

Molecular carbon emission was measured to demonstrate the capability of F^2-LAMIS at long distances. The samples were isotopically enriched ^{13}C graphite samples. The study of ^{13}C is important to climate change, coal combustion and plant research.

We optimized the experimental conditions to obtain ^{13}C isotopic information from the graphite samples. The Swan C_2 and violet CN systems were selected for analysis [3,17-20]. **Figures 4 (a-c)** show the CN molecular band progression using the graphite samples. The vibrational bands corresponding to the violet system (B→X; Δv=1, Δv=0 and v=-1) are clearly visible. **Figures 4 (d-f)** show part of the C_2 emission Swan system for (B-X; Δv=1, Δv=0 and Δv=-1). All these spectra are well resolved and can be used for F^2-LAMIS analysis. The detection gate was set at 0.1μs delay time with a 0.5 μs gate width. The laser repetition rate was set at 200 Hz, with a total accumulation of 1200 pulses/per spectrum (or 6 s/spectrum). The plots shown in **Figure 4** are the average of 50 spectra acquired over a total time of 5 min.

Quantification in LAMIS (or LIBS) generally requires matrix-matched standards to get a prediction model. However, standards are not available real-world in remote sensing applications. An alternative approach for quantification is to use a spectral fitting algorithm to determine the ^{13}C abundance with LAMIS [20]. The rotational and vibrational energy levels of a molecule change when replacing an atom with its isotope. A direct consequence of this, is a change in the corresponding emission wavelengths. This allows isotopes of molecules such as C_2 and CN to be determined from molecular spectra. A computed synthetic spectrum was obtained based on comparing experimentally measured intensity with calculated line intensity for each line position, assuming the existence of thermal equilibrium among rotational and vibrational states. Details of this algorithm can be found elsewhere [20].

Figure 5 shows the molecular spectra of the CN violet system (B→X; Δv=-1, **Figure 5a**), and C_2 Swan system (B→X; Δv=1, **Figure 5b**) and (B→X; Δv=-1, **Figure 5c**) using graphite samples with varying ^{13}C abundance from 1.1% to 6.2 %. These three molecular systems showed a

significant signal response with the increase of ^{13}C concentration. Out of those, the C_2 Swan system at 474.45 μm was selected for quantification using spectral line fitting. This band has the best sensitivity for the $^{13}C^{12}C$ isotopologue with the minor isotope shifted to red and minimal spectral interference with $^{12}C^{12}C$ bands.

Figure 6 presents the spectral measurements of the $^{13}C/^{12}C$ isotopologue in graphite samples having 1.1% to 6.2 % ^{13}C abundance. The figure shows experimental and fitted spectra using the algorithms we previously developed for carbon [17]. The abundance calculated using the synthetic spectra shows fairly good agreement with the reference values, with relative bias ranging from 0.9-10% (**Table 1**). The fitted spectra provide a rotational temperature around 4600 K that is comparable to the previously reported 3870-4125 K range obtained using the Boltzmann plot method for the C_2 swan system in graphite samples [26].

Conclusion

We demonstrated the use of F^2-LAMIS for the remote detection and standardless quantification of isotopes from solid samples at a distance of 36 m. These measurements represent the longest distance so far reported for isotope detection with this technology. Control of the femtosecond filament and plasma generation was achieved by combination appropriately selected spatial, temporal and energy characteristics of the femtosecond laser, and was guided by theory followed by experimental optimization. The characteristics of the filament-induced ablation crater were studied in detail and demonstrated that the interaction depth was of the order of only a few nanometers per pulse. The molecular emission from isotopically enriched carbon samples served

as the basis for the F^2-LAMIS isotopic measurements. Spectral fitting enabled measurement of the $^{13}C/^{12}C$ isotope ratio without the use of calibration standards. The characteristics of this system, such as relatively low pulse energy, portable spectrometer, and fast isotopic signature acquisition time underline the potential of this technology for field applications. The ability to not only detect, but also quantify isotopic ratios at varying low isotopic abundances opens the possibility for the use of portable F^2-LAMIS systems for routine isotope ratio measurements in a number of remote sensing applications.

Acknowledgement

This research was supported by the US Department of Energy, Office of Defense Nuclear Nonproliferation Research and Development under contract number DE-AC02-05CH11231 at the Lawrence Berkeley National Laboratory.

References

[1] R. Russo, X. Mao and O.V. Borisov. ‘‘Laser Ablation Sampling’’. Trends Anal Chem. 17, (1998) 461-469.

[2] R.E. Russo, A. Bol'shakov, X. Mao, C.P. McKay, D.L. Perry, O. Sorkhabi, Laser ablation molecular isotopic spectrometry, Spectrochim. Acta Part B At. Spectrosc. 66 (2011) 99–104.

[3] A. A. Bol’shakov, X. Mao, J. González, R. E. Russo, Laser ablation molecular isotopic spectrometry (LAMIS): Current state of the art. J. Anal. At. Spectrom. 31 (2016) 119-134.

[4] J. J. Laserna, R. Fernández-Reyes, R. González, L. Tobaria, P. Lucena, Study on the effect of beam propagation through atmospheric turbulence on standoff nanosecond laser induced breakdown spectroscopy measurements, Opt. Express, 17 (2009) 10265-10276.

[5] S. L. Chin, Femtosecond Laser Filamentation, Springer Series on Atomic, Optical, and Plasma Physics 55, 2010, Springer NY, USA.

[6] W. Liu, S. L. Chin, Direct measurement of the critical power of femtosecond Ti:sapphire laser pulse in air, Opti. Express, 13 (2005) 5750-5755.

[7] G. Fibich, Y. Sivan, Y. Erlich, E. Louzon, M. Fraenkel, S. Eisenmann, Y. Katzir, A. Zigler, Control of the Collapse Distance in Atmospheric Propagation, Opt. Express, 14 (2006) 4946-4957.

[8] J. H. Marburger, Self-focusing: Theory, Prog. Quant. Electr., 4 (1975) 35-110.

[9] K. Stelmaszczyk, P. Rohwetter, G. Mejean, J. Yu, E. Salmon, J. Kasparian, R. Ackermann, J. P. Wolf and L. Woste, Long distance remote laser-induced breakdown spectroscopy using filamentation in air, Appl. Phys. Lett., 85 (2004) 3977-3979.

[10] P. Rohwetter, K. Stelmaszczyk, L. W¨oste, R. Ackermann, G. M´ejean, E. Salmon, J. Kasparian, J. Yu and J.-P. Wolf, Filament-induced remote surface ablation for long range laser-induced breakdown spectroscopy operation, Spectrochim. Acta, Part B, 60 (2005) 1025-1033.

[11] W. Liu, H. L. Xu, G. M´ejean, Y. Kamali, J.-F. Daigle, A. Azarm, P. T. Simard, P. Mathieu, G. Roy and S. L. Chin, Efficient non-gated remote filament-induced breakdown spectroscopy of metallic sample, Spectrochim. Acta, Part B, 62 (2007) 76-81.

[12] H. L. Xu, P. T. Simard, Y. Kamali, J.-F. Daigle, C. Marceau, J. Bernhardt, J. Dubois, M. Châteauneuf, F. Théberge and G. Roy, Filament-induced breakdown remote spectroscopy in a polar environment, Laser Phys., 22 (2012) 1767-1770.

[13] H. L. Xu, W. Liu and S. L. Chin, Remote time-resolved filament-induced breakdown spectroscopy of biological materials, Opt. Lett., (31) 2006, 1540-1542.

[14] H. L. Xu, G. M´ejean, W. Liu, Y. Kamali, J.-F. Daigle, A. Azarm, P. T. Simard, P. Mathieu, G. Roy, J.-R. Simard, Remote detection of similar biological materials using femtosecond filament-induced breakdown spectroscopy, Appl. Phys. B: Laser Opt., 87 (2007) 151-157.

[15] H. Hou, G. Chan, X. Mao, R. Zheng, V. Zorba, R. Russo, Femtosecond Filament-Laser Ablation Molecular Isotopic Spectrometry, Spectrochim Acta Part B, 113 (2015) 113-118.

[16] K. C. Hartig, I. Ghebregziabher, I. Jovanovic, Standoff Detection of Uranium and its Isotopes by Femtosecond Filament Laser Ablation Molecular Isotopic Spectrometry, Sci. Rep., 7 (2017) 1-8

[17] A. Bol'shakov, X. Mao, J. Jain, D.L McIntyre, R. E. Russo, Laser ablation molecular isotopic spectrometry of carbon isotopes, Spectrochim. Acta Part B, 113 (2015) 106-112.

[18] M. Dong, X. Mao, J.J. Gonzalez, J. Lu, R.E. Russo, Carbon isotope separation and molecular formation in laser-induced plasmas by laser ablation molecular isotopic spectrometry, Anal. Chem. 85 (2013) 2899–2906.

[19] R.E. Russo, D.L. Perry, A. Bol'shakov, X. Mao, Laser Ablation Molecular Isotopic Spectrometry for Rare Isotopes of the Light Elements, Spectroscopy, 29 (2014)

[20] M. Dong, G. Chan, X. Mao, J.J. Gonzalez, J. Lu, R.E. Russo, Elucidation of C2 and CN formation mechanisms in laser-induced plasmas through correlation analysis of carbon isotopic ratio. Spectrochim. Acta Part B, 114 (2014) 30-39.

[21] S. A. Brooke, P.F. Bernath, T. W. Schmidt, G. B. Backay, Line strengths and updated molecular constants for the C2 Swan system, J. Quant. Spectrosc. Radiat. Transf. 124 (2013) 11-320.

[22] C. G. Parigger, A. C. Woods, D. M. Surmick, G. Gautam, M. J. Witte, J.O Hornkohl, Computation of diatomic molecular spectra for selected transitions of aluminum monoxide, cyanide, diatomic carbon, and titanium monoxide, Spectrochim. Acta Part B, 107 (2015) 132-138.

[23] M. Weidman, K. Lim, M. Ramme, M. Durand, M. Baudelet, M. Richardson, Stand-off filament-induced ablation of gallium arsenide, Applied Physics Letter, 101 (2012) 034101-034103.

[24] R. Moser, M. Domke, H. P. Huber, G. Marowsky, Single pulse femtosecond laser ablation of silicon - A comparison between experimental and simulated two-dimensional ablation profiles, Advanced Optical Technologies. 7 (2018) 1-10.

[25] Y. Ma, X. Lu, T. Xi, Q. Gong, J. Zhang, Widening of long-range femtosecond laser filaments in turbulent air, J. Anal. At. Spectrom. 16 (2008) 8332-8341.

[26] E. J. Judge, G. Heck, E. B. Cerkez, R. J. Levis, Discrimination of Composite Graphite Samples Using Remote Filament-Induced Breakdown Spectroscopy, Anal. Chem., 81(2009), 2658-2663.

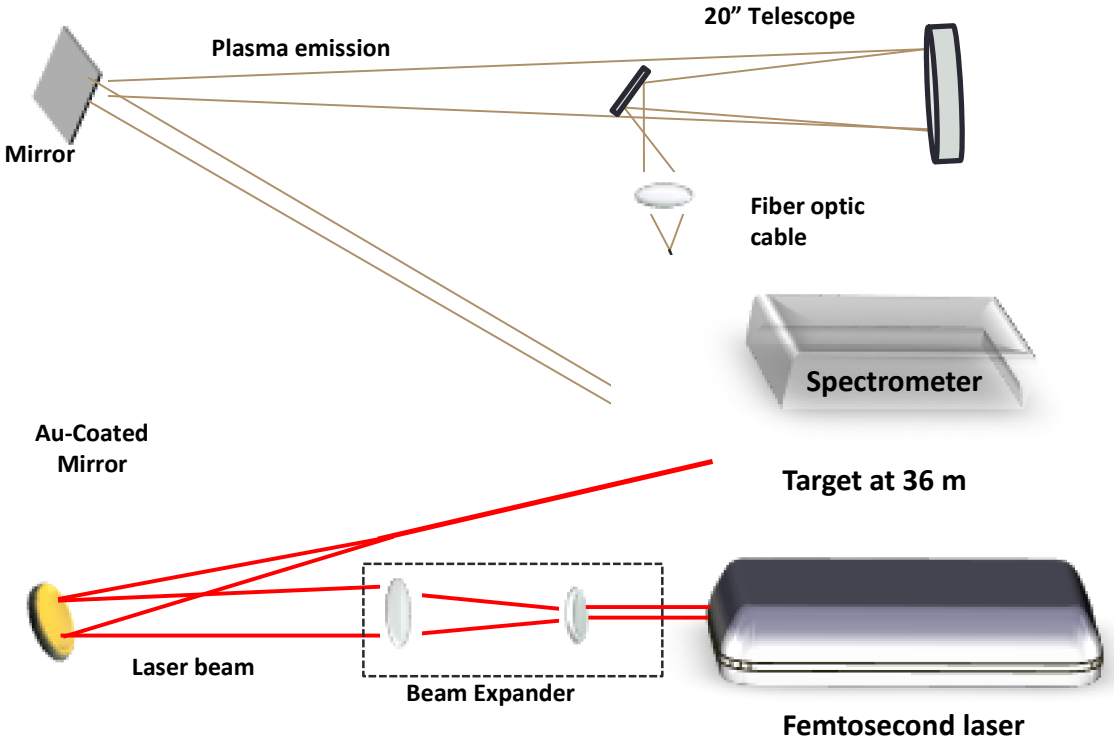

Figure 1. Experimental set up for long distance F^2-LAMIS measurements.

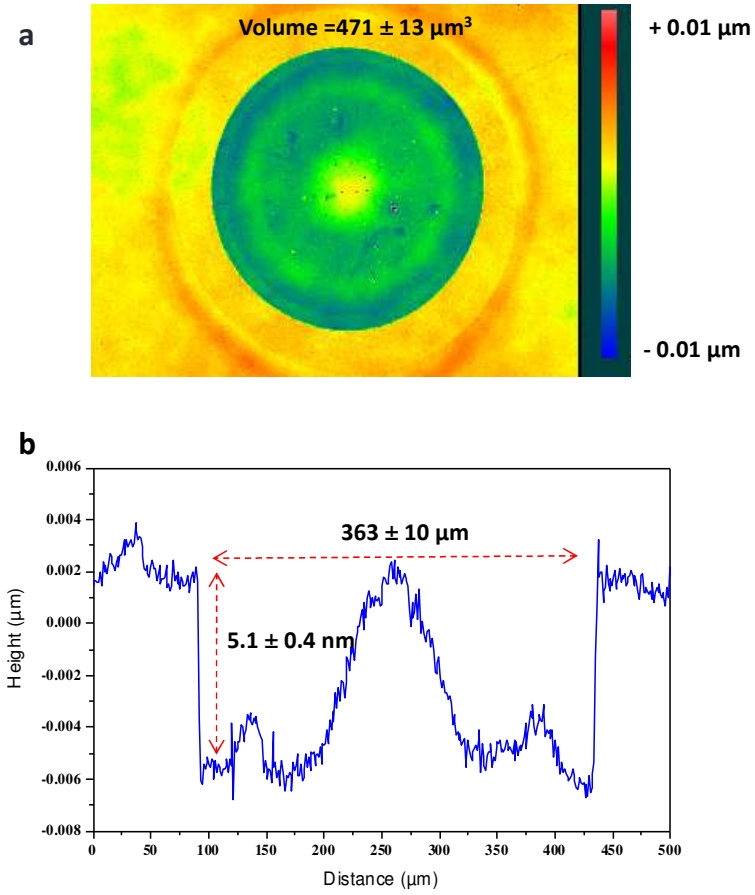

Figure 2. White light interferometry of Si craters obtained using one femtosecond filament pulse. (a) 2D surface plot of the crater morphology and (b) cross-sectional profile at the center of the filament. The color scale in (a) represents the ablation depth.

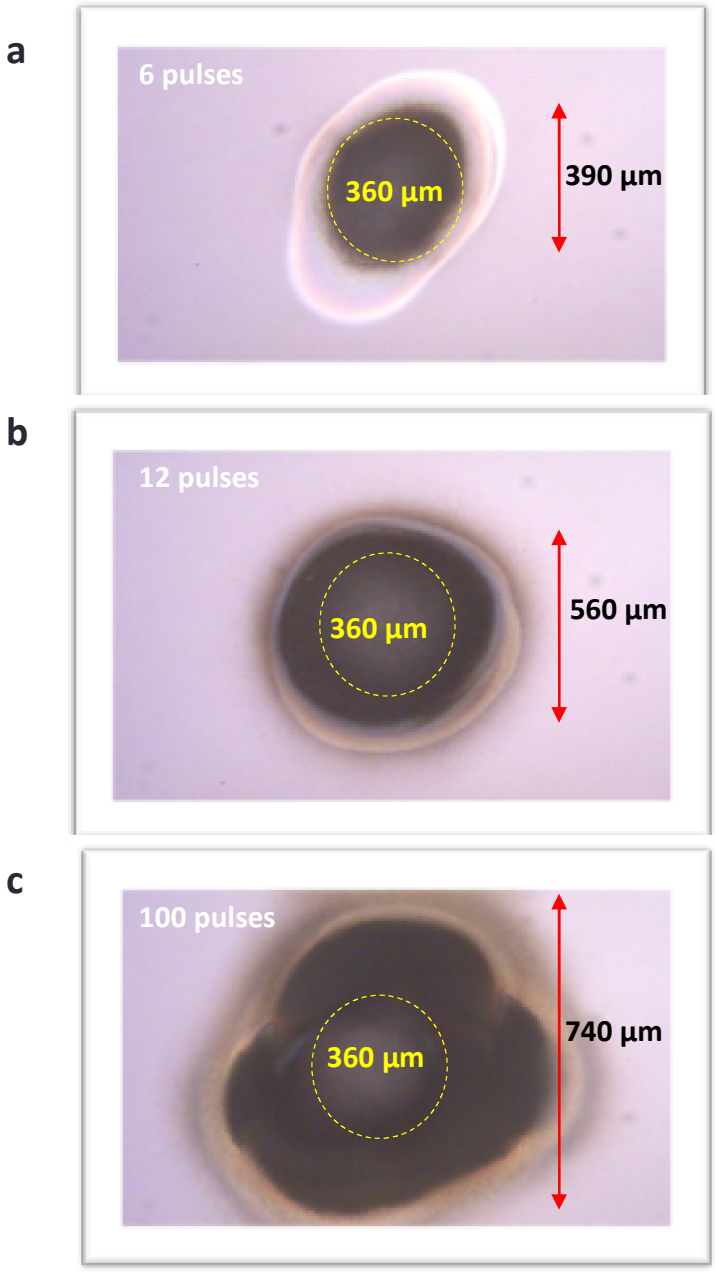

Figure 3. Surface morphology of craters formed on a Si wafer at 36 m by femtosecond laser filamentation with (a) 6, (b) 12 and (c)100 pulses. The filament pointing stability is shown by multiple femtosecond filament ablation spots on the Si surface obtained with consecutive number of pulses.

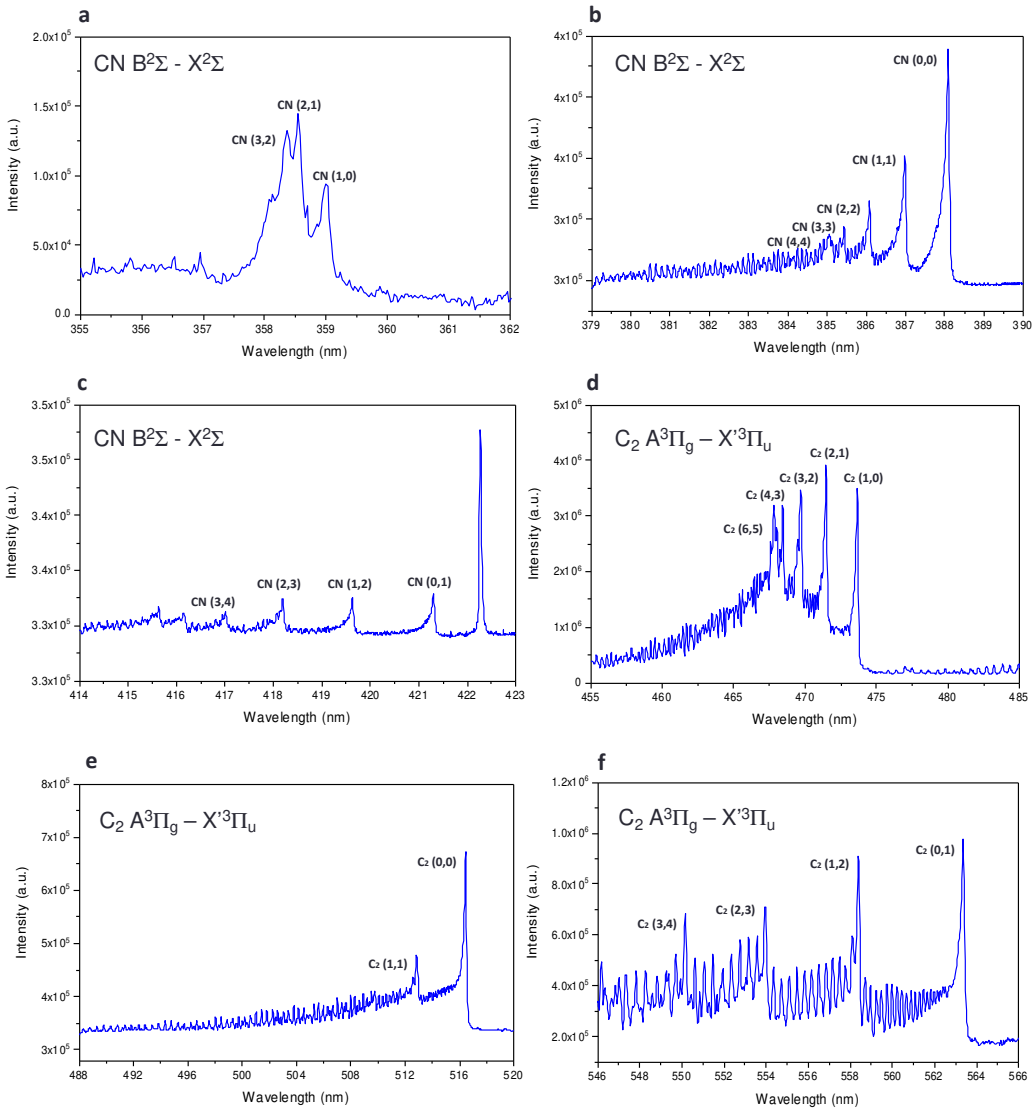

Figure 4. CN and C_2 molecular emission from femtosecond filament plasmas at 36 m. (a-c) the CN B→X; Δν=1, Δν=0 and ν=-1 systems and (d-f) C_2 emission B-X; Δν=1, Δν=0 and Δν=-1. Figures show the average of 50 spectra, each obtained with 1200 pulses at 200 Hz.

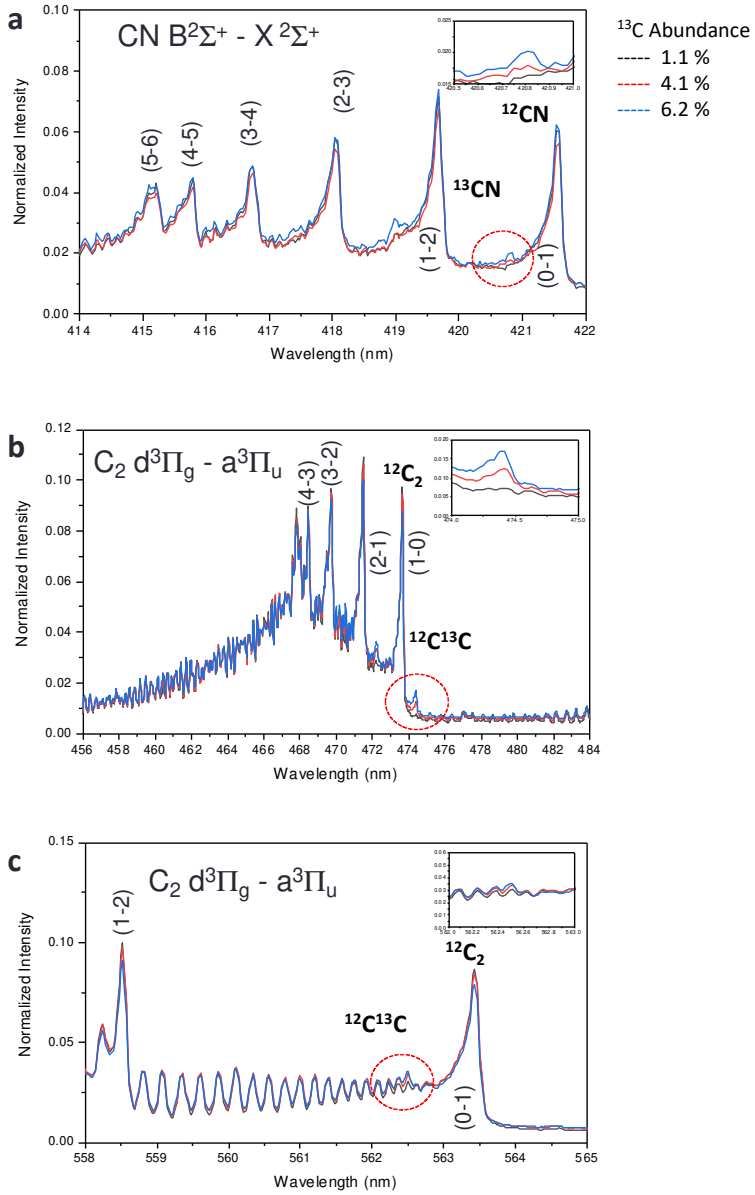

Figure 5. Molecular carbon emission and LAMIS spectra of graphite for different ^{13}C abundance samples using femtosecond filaments at 36 m. a) CN violet system of B→X; Δv=-1. b-c) C_2 spectra of B→X; Δv=1 and B→X; Δv=-1. Figures show the average of 50 spectra, each obtained with 1200 pulses at 200 Hz. The insets correspond to the area indicated by the circle.

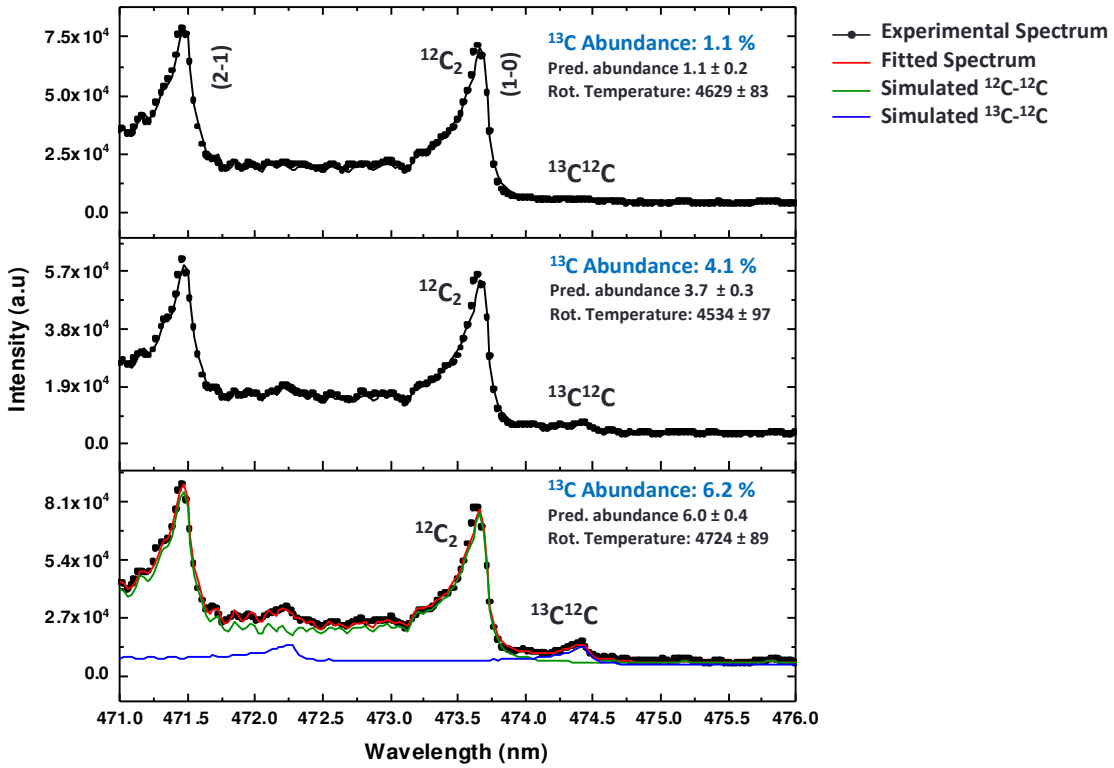

Figure 6. Experimental and simulated F^2- LAMIS of C_2 using Swan $\Delta v = +1$ system. The ^{13}C reference isotopic abundances were 1.1, 4.1 and 6.2%, respectively. Figures show the average of 5 spectra obtained with 1200 pulses at 200 Hz. The error in the predicted abundance was obtained with ten replicates of the experimental spectra.

Table 1. ^{13}C isotopic abundance for isotopically enriched graphite samples. Reference values, predicted values by standardless approach using simulated spectra, and relative bias.

^{13}C Reference Value, %	**^{13}C Predicted Value, %**	**Relative Bias,%**
1.11	1.1 ± 0.2	-0.9
4.11	3.7 ± 0.3	- 10.0
6.21	6.0 ± 0.4	- 3.9

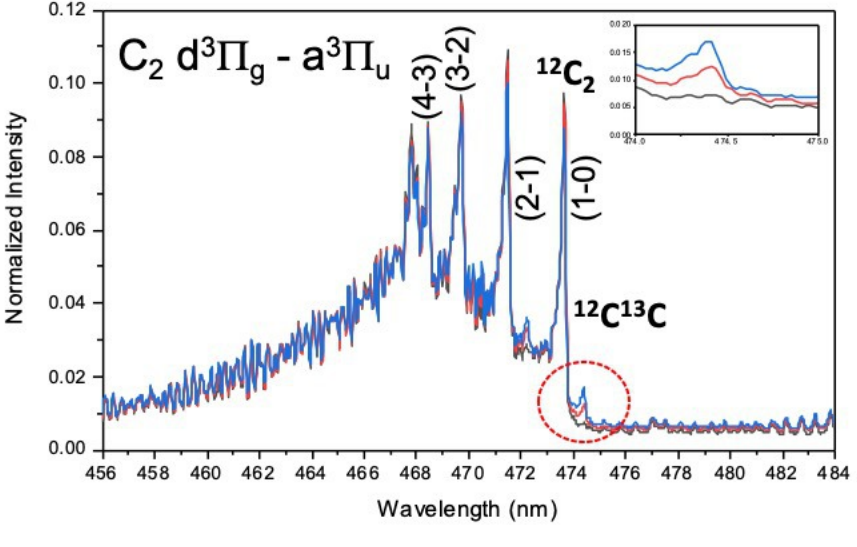
C2 d3Πg - a3Πu
(4-3)
(3-2)
(2-1)
(1-0)
12C2
12C13C
Normalized Intensity
Wavelength (nm)
0.12
0.10
0.08
0.06
0.04
0.02
0.00
456
458
460
462
464
466
468
470
472
474
476
478
480
482
484